RESIDUAL STRESSES AND FRACTURE TOUGHNESS BORIDE CERAMIC COMPOSITES WITH MONOCRYSTALLINE MATRIX

[1]Soloviova T.O., [1]Loboda P.I., [2]Karasevska O.P., [1]Samsonik I.V.
[1]National Technical University of Ukraine "KPI", Peremohy Av. 37, 03680 Kyiv, Ukraine
[2]Institute Metal Physics. G.V. Kurdyumov Sciences of Ukraine, blvd.Acad. Vernadskogo 36, 03680 Kyiv, Ukraine

E-mail: tsolov@iff.kpi.ua

Abstract: *X-ray diffraction analysis studies the formation of a stress-strain state of single-crystal composites LaB_6-TiB_2 obtained under identical conditions by crucible-free float zone melting (FZM). The composites were obtained using monocrystalline LaB_6 substrate seeds with <100>, <110> and <111> orientations. It is shown that indentation-induced deformation in the composite materials obtained by FZM is distinct from the deformation expected in their equilibrium state. This difference arises in part from residual thermal strains in both phases of the composites in a FZM -grown state. Interplay between residual thermal deformations and external mechanical deformation results in a complex distribution of dilatational strain in the LaB_6 matrix and TiB_2 fibers and differs in composites of different orientations. Reversal sign of the stress-strain state (e.g., alternating tensile/compressive/tensile in central part of the cross-section area) is observed predominantly in the matrix LAB_6 and the TiB_2 fibers of the composite with the orientation <111>. In the composite with the orientation <100>, this change in the deformation sign was not observed. The size and spread of cracks after indentation-induced deformation shows a decrease in microhardness in FZM -grown composites of <111> significantly more (40%) than in composites with a orientation of <100> (10%) compared with an equilibrium state.*

Keywords: BORIDE COMPOSITE, FRACTURE TOUGHNESS, DIRECTIONAL SOLIDIFICATION, RESIDUAL STRESSES, EUTECTIC ALLOY, MONOCRYSTALLINE STRUCTURE

1. Introduction

Progress of the technologies for receiving composite materials by directionally solidification including floating zone method (FZM) allowed significantly improved the mechanical properties of single crystals and composites [1-4]. The FZM process are characterized by significant temperature gradients along and perpendicular to the direction of movement of the melting zone and cause residual stresses (RS) in the matrix and fibers of composite. Previous studies [4,8 -10] also show that the strength and plasticity of the directionally solidified LaB_6–MeB_2 (Me–Ti, Zr, Hf) eutectics depends on the crystallographic orientation of the matrix phase (LaB_6). On the mechanical characteristics of composites with a reinforcing phase in the form of fibers, the decisive influence is the interface boundary, that is, the strength of the adhesion of fibers with the matrix. Under the interface boundary in this case, it is understood not only the geometric [5] surface of the separation between fibers and the matrix, but also adjacent to it areas, which are affected by the influence of physicochemical and thermomechanical processes occurring in the stages of formation of the composite.

It is believed [11] that for the mechanical characteristics of composites with a reinforcing phase in the form of fibers, the decisive influence is the interface boundary, that is, the strength of the adhesion of fibers with the matrix. Under the interface boundary in this case, it is understood not only the geometric surface of the separation between fibers and the matrix, but also adjacent to it areas, which are affected by the physicochemical and thermomechanical processes occurring at the composites stages formation. The morphology of the phases formed during the FZM depends on a number of factors, but the most important is the ratio of the rate of their origin and growth, which in turn depends to a large extent on the thermal conditions and the supercooling at the crystallization front. Under the interface boundary in this case, it is understood not only the geometric surface of the separation between fibers and the matrix, but also adjacent to it areas, which are affected by the physicochemical and thermomechanical processes occurring at the composites stages formation.

The technological experimental parameters of the FZM process: the velocity of the melting zone, the temperature gradient values, the shape of the crystallization front provides conditions for the formation of nucleus (nucleation) of different orientations. Growth of grains with crystallographic orientation [001] according to the model [12] there is an advantage, since they occur at the slightest supercooling. Under the same conditions of crystallization, composites with different orientations of the seeds will have different conditions in terms of the competitive growth of the nucleus at the crystallization front. As a result of the directionally FZM method the thermal RS occur in both phases and are described by the stress tensor [13]. With a uniform action of external forces, internal stresses are described by a symmetrical stress tensor with only diagonal terms. The non-coincidence of the directions of preferential growth and the maximum temperature gradient leads to the fact that the stress tensor becomes asymmetric, i.e. shear, tangential stresses are present in the material. The sign of the acting force (RS) on the environment on the composite side is opposite to the sign of the external force (temperature gradient) acting on the composite.

The RS sign determines their effect on fracture propagation with an additional mechanical effect on the composite. Investigation the crack spread under the indent is the main testing in LaB_6-based ceramics to characterize a stress-strain state [9, 14-17]. Internal RS measurements have already been performed in ceramic eutectics using either X-ray or neutron [9, 17–21] diffraction techniques.

The aim of the experiment was to establish the interrelation between cracks propagation and stress-strain state of LaB_6-TiB_2 composites obtained on the seeds with different orientations by the FZM method.

2. Experimental procedure

The LaB_6 and TiB_2 powders (purity 98 wt. % , average grain size 1 μm, Reaktiv Co Donetsk, Ukraine) were mixed in the eutectic, 89 wt. % LaB_6 and 11 wt. % TiB_2, composition. In order to assist the purification of the starting powder mixture during crucible-free FZM, 2 vol. % amorphous boron (purity 99.8 wt%, particle size 0.5 μm, Reaktiv Co Donetsk, Ukraine) powders was admixed. 15 ml of a 2.5 wt% polyvinyl alcohol aqueous solution was used as binder per 100 g of powder mixture. After mixing by 10 times manual wet sieving through a 100 μm mesh sieve, the dried powder mixture was sieve granulated (1000 mm mesh) and uniaxial pressed in a hydraulic press at 100 MPa in a steel cylindrical mold with a working cavity diameter of 10 mm and length of 145 mm. Directionally reinforced LaB_6–TiB_2 composites were obtained by the original floating zone method, developed at the National Technical University of Ukraine (NTUU “Igor Sikorsky KPI”). FZM was performed at a speed of 3 mm/min in the "Crystal 206"(Russia) induction equipment in a 0.1 MPa helium

WEB ISSN 2535-0226
PRINT ISSN 2535-0218

environment using single crystal LaB_6 substrate seeds with <100>, <110> and <111> orientations. 5-6 samples for studies were cut perpendicular to the axis of the central part of each cylindrical crystal. The disks (d = 8 mm, h = 6-8 mm) were polished with diamond suspensions of 15 and 3 μm. Microstructure investigation of the composites was performed by scanning electron microscopy (PEM 106I). X-ray diffraction investigations were produced on a XRD diffractometer (Ultima IV, Rigaku, Japan) using $Cu_{K\alpha}$ radiation, a 2Θ step size of 0.02° and measuring time of 2s/step. The RS in different planes were determined by the sin2Θ method. To reduce the error in the determination of RS (up to <20-25%) measurements were made on ~10 different sample regions and with their inclination in opposite directions. The microhardness was measured by Vickers pyramidal indentation (MHV-1000 microhardness tester with time exposure 15 s, and averaging 7 measurements under a load of 30N. The fracture toughness on the transverse cross-section was computed from the Vickers hardness, using the expression proposed by Evans and Charles for Palmqvist cracks [22].

3. Results and discussion

The distribution of intensity on "Θ-2Θ" X-ray diffraction patterns and pole figures for different LaB_6-TiB_2 composites is shown on fig 1. For composites of all orientations there are reflexes for the matrix phase (LaB_6) and fibers (TiB_2) (Fig 1 a, c, e). The content of the matrix phase is ~ 87-89 wt.% and the fibers are ~ 11-13 wt.%. A significant number of reflexes are observed on the pole figures (Fig. 1 b, d, f) of samples for all orientations. Reflexes with a high intensity in accordance with their positions allow one to determine the preferential orientation of the samples, which repeats the orientation of the substrates. The symmetry of fourth-order for the high intensity reflexes is observed in composite produced on a substrate <100>, and for composites on substrates <110> and <111> there are the second and third orders, respectively. The total intensity of polycrystalline reflexes at the pole figures FZM-grown composites allow us to estimate their volume in ~8-20%. The volume of polycrystalline components of composites depends on the orientation of the substrate and can be reduced during annealing of composites [21]. Polycrystalline constituents of composites are represented on "Θ-2Θ" diffraction patterns (Fig. 1a, c, e) as additional to single-crystal reflexes.

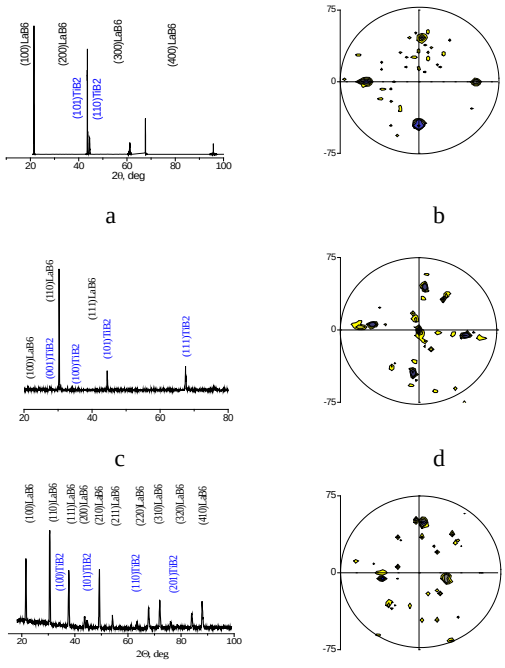

a,b – <100>; c, d – <110>; e, f – <111>

Fig 1. *«θ–2θ» X-ray diffractograms and pole figures matrix components LaB_6 of composite LaB_6-TiB_2*

The significant temperature gradients and difference in the coefficients of thermal expansion leads to the fact that when cooled sintered by FZM composites from temperatures below which the phases cannot be plastically deformed, there is the formation of internal stresses around not only a fibers interface with a larger coefficient of thermal expansion (CTE) compared with the matrix but in the matrix and the fibers. The coefficient of thermal expansion matrix phase LaB_6 is ~6 10-6 K^{-1} [23] and for TiB_2 in c-axis is ~ 9.3 10-6 K^{-1} and in a-axis is ~ 6.35 10-6 K^{-1} [24]. In the equilibrium state LaB_6-TiB_2 composites have only interfacial stresses to which at FZM in conditions of significant temperature gradients added residual macrostresses in the composites components.

The orientation of the seed during the formation of composite materials is also main key factors shaping the residual stresses after FZM. On the Fig. 2 [6] shown the distribution of residual stresses in cross-sections of crystals obtained with different moving speed with orientations of the axes <111> and <100> having symmetries of 3 and 4 orders respectively.

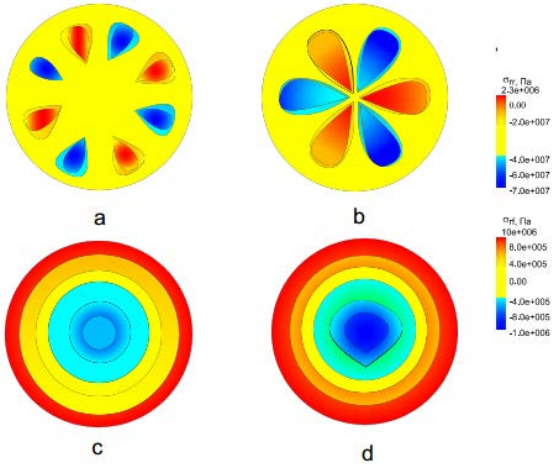

Fig. 2. *Cylindrical stress components σ_{rr} (middle) and $\sigma_{r\phi}$ (bottom) on the crystallization interface of FZM crystals with <100> (a, c) and <111> (b, d) orientation and a growth rate of 2.5 mm/min*

For the orientation of crystals <100>, the lateral surface of the cross sections is in a tensile state while the central part is compressed, which corresponds to a negative value of the shift on the X-ray diffraction patterns. As the crystallization rate decreases, absolute values of residual stresses decrease. The change in the sign of the stresses from the center to the lateral surface is symmetrical and occurs uniformly for any radial direction. In crystals with orientation <111>, a change in the sign of RS along the circumference is observed. As the rate of crystallization decreases, the absolute values of the residual stresses decrease, but the change in the stress sign remains, albeit in a smaller region of the material. The distribution of RS (Fig. 2) in the cross section of single crystals is related to the mutual position of the sliding planes, the direction of preferential growth and the temperature gradient at the crystallization front.

On the X-ray diffraction patterns, this is manifested in a change in the displacement of the reflexes when the slope of the sample is changed, which is used in the "$\sin^2\psi$" method (Fig.3). The leading parameter in analyzing the characteristics of growth is the growth rate. Each type of plane grows at a certain speed. The growth rate is directly proportional to the number of atoms forming the plane, and is calculated as the ratio of the number of atoms entering the plane to the area of the plane, that is, determined by the reticular density. For La atoms, the relative reticular density of the different planes is: {100}: {110}: {111} as 1: 0.707: 0.650.

In Fig.3, for disk samples of composites {100} (Fig.3a) and {111} (Fig.3b), the change of the RS in different planes is shown. Differences in the RS values significantly exceed the measurement error. In composites {100} a different level of compressing RS is

WEB ISSN 2535-0226
PRINT ISSN 2535-0218

observed in different planes and for all planes in the cross-section are dominated by compression stresses. In the composite {111}, not only different levels of RS are observed in the planes, but also different signs of these RS. It is very important to note that in the matrix phase of the composite in different directions, a different sign is formed. The complex-stress state is characteristic for composites obtained by FZM process.

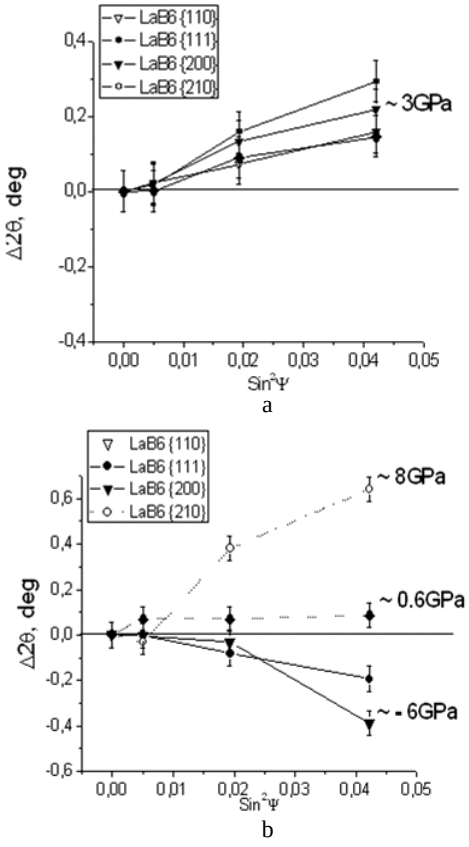

Fig 3. *The residual macrostresses in various planes of the matrix phase of the composites <100> (a) and <111> (b), which are determined by the $\sin^2\psi$ method on the transverse sections of the samples*

The residual stresses significantly affect the mechanical behavior of the material. Concerning the crack propagation modes, tensile stresses within a phase will act in favor of transverse crack propagation in this phase, whereas a normal tensile stress on the phase boundaries will help the interface crack propagation [9, 14-17]. Interplay between RS and external mechanical deformation (indentation of a pyramid) results in a complex distribution of dilatational strain in the LaB_6 matrix and TiB_2 fibers and differs in composites of different orientations. This interaction is manifested in the peculiarities of the propagation of cracks. In Fig.4 shows the microstructures of composites with pyramid indentation obtained on substrates with orientations of {100}, {110} and {111}. Common for cracks in composites of all orientations due to the indentation of the pyramid is their formation and stopping in the matrix phase, enveloping the reinforcing fibers and not penetrating the matrix-fiber interface. The peculiarities of the appearance of cracks in composites of different orientations are the regions of generation and the directions of their propagation relative to the diagonals of the indentation. In the {100} composites cracks originate from the tops of indentation area and extend in the direction of their diagonals, corresponding to the places and directions of the maximum load (Fig.4a). The microstructure of the {111} composite in the region of the indentation with cracks is shown in Fig.4b. In the area of indentation, we can distinguish several grains that easily differ in the position of the fibers in them (Fig.4c). Cracks are generated and propagated in any direction relative to the maximum load (diagonals of the indentation) and the melting direction of the zone.

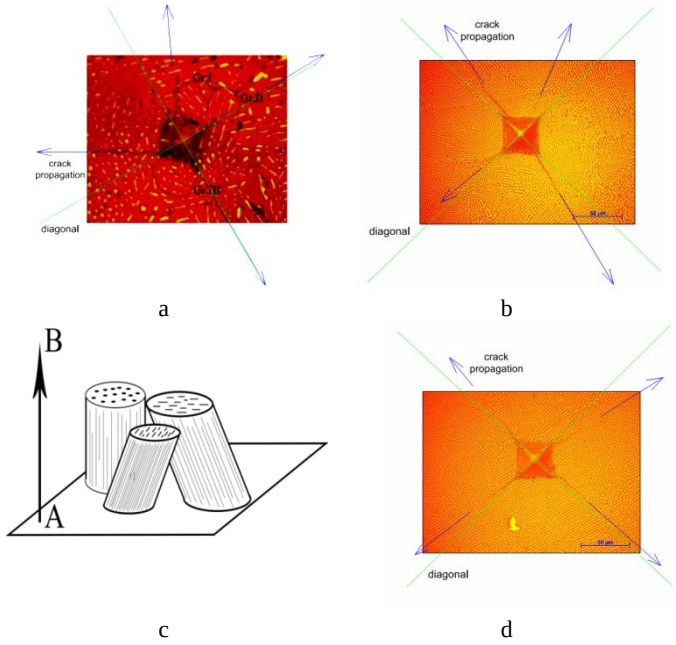

Fig 4. *Typical microstructures indentations (a, b, d) in composites with orientations <111> (a), <110> (b), <100> (d) and scheme grains structure in composite <111> (c); directions of cracks propagation (blue lines) and diagonals indentations (green lines), AB - direction of the maximum temperature gradient*

The distribution of cracks indicates the existence of regions with a lighter and more difficult motion in the matrix phase. In composites with these orientations, RS of different signs were found, which leads to the formation of a complex stress state. The measurement of the crack length after Vickers indentation (tab. 1) shows very strong anisotropy for single crystals with different direction of crystallization.

Table 1 – *Anisotropy crack length in the single crystals LaB_6-TiB_2 composite after FZM*

Direction of crystallization	<100>	<110>	<111>
Anisotropy of crack length, %	7.8	29.7	41.5

To the anisotropy of the coupling of the atoms of lanthanum and boron in the matrix LaB_6 and taking the interaction between the matrix and the fibers is added to the complex stress-strain state arising as a result of FZM process.

4. Conclusions

In ceramic composites produced by FZM, residual stresses are formed, which determine their crack resistance. In the cross sections of composites obtained in seedlings with different reticular densities, different residual stresses are observed not only in magnitude but also in sign. When using the seed {111}, the matrix phase of the composite is in a complex stressed state with an inhomogeneous distribution of residual compressive and tensile stresses. The larger the reticular density, the greater the rate of equilibrium crystallization and the more homogeneous RS are observed. Conversely, the smaller the reticular density, the lower the rate of equilibrium crystallization and the more complex the stress state is formed in the composites. The same rate of crystallization of composites of different orientations occurs with different supercooling and bending at the crystallization front. The

deviation of the direction of the preferential growth of the crystal from the maximum temperature gradient leads to additional deformations of the composites.

5. References

1. H. Bei, E.P. George, Microstructures and mechanical properties of a directionally solidified NiAl–Mo eutectic alloy, *Acta Materialia*, Vol. 53 (2005), p. 69–77.

2. V. M. Orera, I. Merino, A. Pardo and etc., Microstructure and physical properties of some oxide eutectic composites processed by directional solidification, *Acta mater.*, Vol. 48 (2000), p. 4683–4689.

3. R.S. Bradt, V.S. Stubican, Eutectic solidification in ceramic systems, *Ann. Rev Mater. Sci*., Vol. 11 (1981), p. 267–297.

4. I. Bogomol, T. Nishimura, O. Vasylkiv and etc., High-temperature strength of directionally reinforced LaB_6–TiB_2 composite, *J. of Alloys and Compounds*, Vol. 505 (2010), p. 130–134.

5. Q. Ren, H. Su, Ju. Zhang and etc., Directional solidification and growth characteristics of Al2O3/Er3Al5O12/ZrO2 ternary eutectic ceramic by laser floating zone melting, *J. Mater. Sci.*, Vol. 52 (2017), p. 5559–5568.

6. I. Drikis, M. Plate, Ju. Sennikovs and etc., Effect of process parameters and crystal orientation on 3D anisotropic stress during CZ and FZ growth of silicon, *J. of Crystal Growth*, Vol. 12 (2016).

7. A. Augusto, D. Pera, H. J. Choi and etc., Residual stress and dislocations density in silicon ribbons grown via optical zone melting, *J. of Applied Physics*, Vol. 113 (2013), p. 083510-1 - 083510-7.

8. W.-T. Chen, R.M. White, T. Goto and etc., Directionally Solidified Boride and Carbide Eutectic Ceramics, *J. Am. Ceram. Soc.*, Vol. 99 (2016), p. 1837–1851.

9. I. Bogomol, T. Nishimura, Yu. Nesterenkoa ant etc., The bending strength temperature dependence of the directionally solidified eutectic LaB_6–ZrB_2 composite, *J. of Alloys and Compounds*, Vol. 509 (2011), p. 6123–6129.

10. Yu. Paderno, V. Paderno, V. Filippov, Some Peculiarities of Eutectic Crystallization of LaB_6–$(Ti,Zr)B_2$ Alloys, *J. Solid State Chem.*, Vol. 154 (2000), p. 165–167.

11. H. Volkova, V. Filipov, Yu. Podrezov, The influence of Ti addition on fracture toughness and failure of directionally solidified LaB_6–ZrB_2 eutectic composite with monocrystalline matrix, *J. of the European Ceramic Society*, Vol.14 (2014), p. 3399-3405.

12. D.Walton, B. Chalmers, The origin of the preferred orientation in the columnar zone of ingots, *Transaction of AIME*, Vol. 215 (1959), p. 447-452.

13. L.D Landau,. E.M. Lifshitz, Theory of elasticity, Oxford ; New York : Pergamon Press, 1970, 168 p.

14. P.I. Loboda, Features of Structure Formation with Zone Melting of Powder Boron-Containing Refractory Materials, *Powder Metall. Met. Ceram.*, Vol. 39 (2000), p. 480–486.

15. H. Deng, E.C. Dickey, Y. Paderno and etc., Crystallographic characterization and indentation mechanical properties of LaB_6-ZrB_2 directionally solidified eutectics, *J. Mater. Sci.*, Vol. 39 (2004), p. 5987–5994.

16. Yu. Paderno, V. Paderno, V. Filippov, Directionally Crystallized Ceramic fiber-Reinforced Boride Composites, *J. Solid State Chem.*, Vol. 154 (2000), p. 165–167.

17. G.E. Ice, R.I. Barabash In: Nabarro FRN, Hirth JP, Strain and Dislocation Gradients from Diffraction: Spatially-Resolved Local Structure and Defects, *Dislocations in solids*, Vol. 13 (2007), p. 500–60.

18. E.C. Dickey, C.S. Frazer, T.R. Watkins and etc. Residual stresses in high-temperature ceramic eutectics, *J. Eur. Ceram. Soc.*, Vol. 19 (1999), p. 2503–2509.

19. H. Suzuki, K. Akita, Y. Yoshioka and etc., Evaluation of phase stresses of Al sub 2 O sub 3 /YAG binary MGC by synchrotron radiation. Residual stress states and stress behavior of YAG phase, *J. Soc. Mater. Sci. Jpn.*, Vol. 52 (2003), p. 770–775.

20. S. Torii, T. Kamiyama, K. Oikawa and etc., Strain measurement of the directionally solidified eutectic Al2O3/Y3Al5O12 (YAG) ceramic by neutron diffraction, *J. Eur. Ceram. Soc.*, Vol. 25 (2005), p. 1307–1311.

21. P.I.Loboda, O.P. Karasevska, T.O. Soloviova, Mode of Deformation of Phase Components of a Ceramic Composite LaB_6-TiB_2, *Metallofiz. Noveishie Tekhnol*., Vol. 38 (2016), p. 1249-1263 (in Ukrainian).

22. F. Sergejev, M. Antonov, Comparative study on indentation fracture toughness measurements of cemented carbides, *Proc. Estonian Acad. Sci. Eng.*, Vol. 12 (2006), p. 388–398.

23. N. N. Sirota, V. V. Novikov, V. A. Vinokurov and etc., Temperature dependence of the heat capacity and lattice constant of lanthanum and samarium hexaborides, *Fiz. Tverd. Tela* (St. Petersburg), Vol. 40 (1998), p. 2051–2053.

24. Norihiko L. Okamoto, Misato Kusakari, Katsushi Tanaka and etc., Anisotropic elastic constants and thermal expansivities in monocrystal CrB2, TiB2, ZrB2, *Acta Materialia*, Vol. 58 (2010), p. 76–84.